

# Unusual optical coherence tomography findings resembling sea anemone tentacles after orbital atherectomy for nodular calcification lesions in a haemodialysis patient: a case report

Mayuko Imamura, Kei Yunoki \*, Katsunori Miyahara , and Takefumi Oka

Department of Cardiology, Tsuyama Chuo Hospital, 1756 Kawasaki, Tsuyama, Okayama 708-0841, Japan

Received 20 July 2023; revised 6 February 2024; accepted 15 February 2024; online publish-ahead-of-print 19 February 2024

## Background

Optical coherence tomography (OCT) can be used to characterize the details of calcified plaques because it allows high-resolution evaluation of coronary plaques, thrombi, and calcium.

## Case summary

A 72-year-old man on haemodialysis who had stenosis with a severe calcified lesion at the left anterior descending artery underwent percutaneous coronary intervention. Pre-intervention OCT imaging identified a nodular calcification (NC) that protruded into the lumen of the left anterior descending artery. To treat this lesion, we performed orbital atherectomy using the Diamondback 360 coronary orbital atherectomy system. After ablation of the nodular lesions at low and high speed, OCT showed newly emerged granular and filamentous structures that resembled sea anemone tentacles (these represented calcified nodule-like OCT findings). These structures appeared to extend from the proximal part of the ablated small NC, and shifted distally after balloon dilatation. Stent implantation was performed to entirely cover these structures, with no resulting complications. However, early in-stent restenosis occurred at 4 months follow-up.

## Discussion

A tentacle-like OCT appearance in calcified lesions has not been previously reported. This represents a very rare and interesting imaging finding that reflects the relationship and origins of NCs and calcified nodules. The maturity of the NC lesions and the lateral sanding style of the orbital atherectomy system may have contributed to this striking OCT finding.

## Keywords

Sea anemone tentacle • Optical coherence tomography • Nodular calcification • Orbital atherectomy • Haemodialysis • Case report

## ESC curriculum

2.1 Imaging modalities • 3.1 Coronary artery disease

## Learning points

- Orbital atherectomy system-based debulking of nodular calcified lesions in a haemodialysis patient revealed a very unusual granular and filamentous appearance on optical coherence tomography (OCT) that resembled sea anemone tentacles (this represents a calcified nodule-like OCT finding).
- The sea anemone tentacle-like structures were potentially platelet/fibrin thrombi formed by the mixing of intra-nodal components and blood flow due to debulking.
- Although nodular calcification and calcified nodules are distinctly different pathological lesion morphologies, our findings suggest that both conditions are transitional.

\* Corresponding author. Tel: +81 868 21 8111, Fax: +81 868 21 8201, Email: [kei.yunoki@gmail.com](mailto:kei.yunoki@gmail.com)

Handling Editor: Milenko Zoran Cankovic

Peer-reviewers: Nidhi Madan; Sabeeda Kadavath; Daniel Messiha

Compliance Editor: Zhiyu Liu

© The Author(s) 2024. Published by Oxford University Press on behalf of the European Society of Cardiology.

This is an Open Access article distributed under the terms of the Creative Commons Attribution-NonCommercial License (<https://creativecommons.org/licenses/by-nc/4.0/>), which permits non-commercial re-use, distribution, and reproduction in any medium, provided the original work is properly cited. For commercial re-use, please contact [journals.permissions@oup.com](mailto:journals.permissions@oup.com)

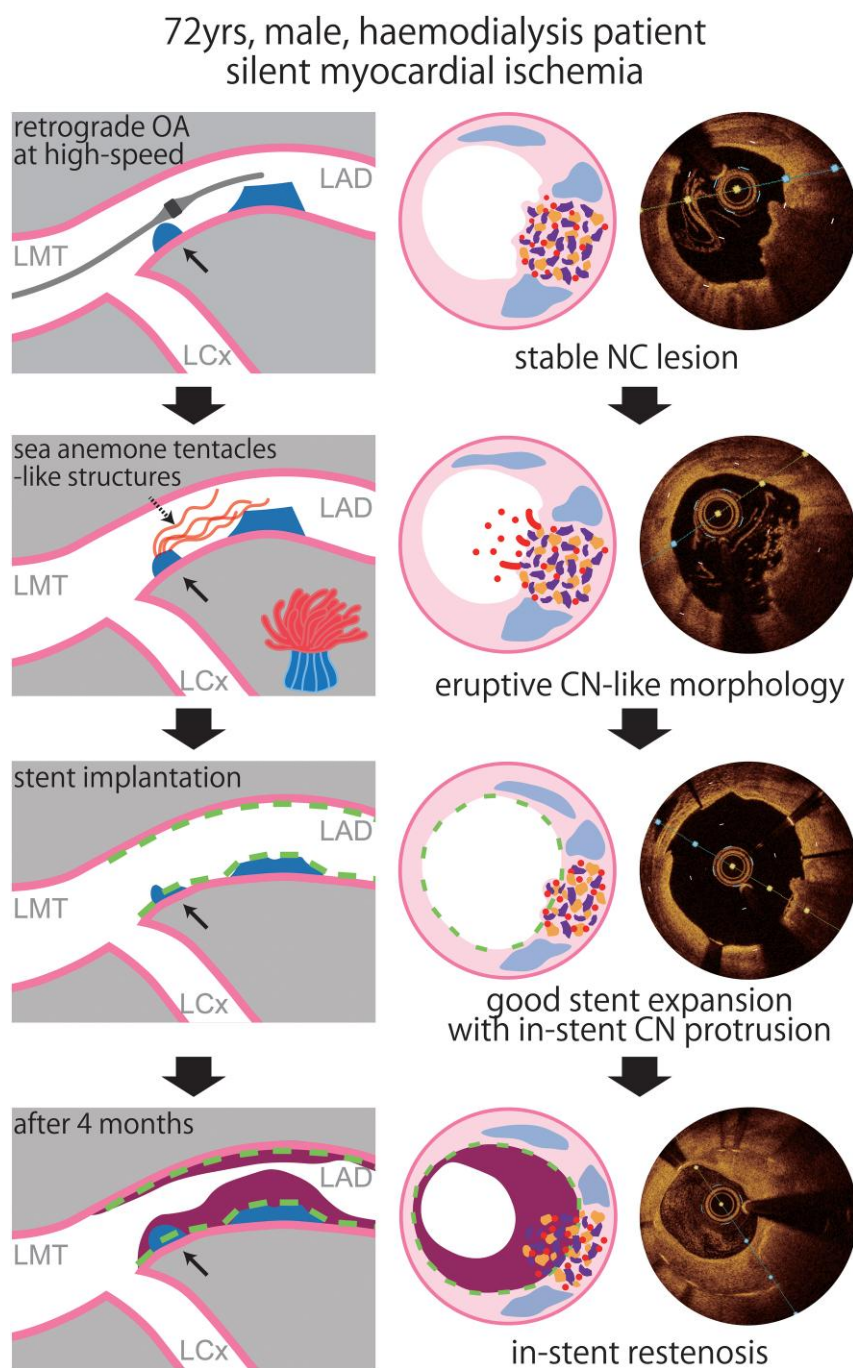
## Introduction

Optical coherence tomography (OCT) provides high-resolution assessment of coronary plaques, thrombi, and calcium deposits. As such, it can be used to characterize the details of calcified plaques, including nodular calcifications (NCs) and calcified nodules (CNs). Nodular calcifications and CNs are characterized by an underlying heavily calcified plaque with a distinct nodular mass of calcium that

protrudes into the lumen. However, unlike NCs, CNs rupture into the lumen and are always associated with a thrombus.<sup>1</sup>

Herein, we report a male haemodialysis patient with NC lesions in the left anterior descending artery (LAD) who underwent debulking using orbital atherectomy. The patient showed very unusual granular and filamentous structures on OCT resembling sea anemone tentacles that appeared to be platelet/fibrin thrombi, which closely resembled a CN.

## Summary figure



## Case presentation

A 72-year-old man was referred to our hospital for bradycardia and hypotension during haemodialysis. He had started maintenance haemodialysis 10 years earlier because of diabetic nephropathy. On physical examination, his consciousness was clear and his blood pressure was 144/80 mmHg, pulse was 27 beats/min with regular rhythm, body temperature was 36.4°C, and oxygen saturation was 94% in room air. Auscultation revealed normal respiratory sounds and a grade 2/6 systolic ejection murmur at the 2nd intercostal space of right border of the sternum, and lower extremity oedema was not observed. Laboratory results indicated an elevation in brain natriuretic peptide levels at 1076.1 pg/mL (normal range:  $\leq 18.4$  pg/mL), but no increase in creatine kinase (CK) at 43 U/L (men: 59–248 U/L, women: 41–153 U/L), CK-MB fraction at 8 IU/L ( $\leq 12$  IU/L), and high-sensitivity cardiac troponin T at 0.074 ng/mL ( $< 0.10$  ng/mL). Chest radiography showed cardiomegaly without pleural effusion. Twelve-lead electrocardiography showed a heart rate of 34 beats/min with complete atrioventricular block. Transthoracic echocardiography revealed left ventricular hypertrophy, but no wall motion abnormality (ejection fraction of 68%), along with a mild level of aortic stenosis, mitral and tricuspid regurgitation. His bradycardia was caused by paroxysmal atrioventricular block. Given the possibility of myocardial ischaemia as the cause of paroxysmal atrioventricular block and hypotension during haemodialysis, a temporary pacemaker was implanted, and simultaneous coronary angiography (CAG) was performed. Coronary angiography showed severe stenosis with eccentric calcified lesions in the proximal LAD ([Figure 1A and B](#)). The stenotic lesion in the LAD was considered stable because there were no chest symptoms or findings on clinical examination that suggested acute coronary syndrome (ACS).

Blood pressure did not decrease during haemodialysis after temporary pacemaker implantation, and dual antiplatelet therapy (DAPT) with aspirin and prasugrel [the standard regimen in percutaneous coronary intervention (PCI) at our hospital and throughout Japan] was initiated after permanent pacemaker implantation. The patient was treated with DAPT for at least 2 weeks, and after confirming the condition of the pacemaker wound and the tolerability of DAPT for bleeding complications, treatment of the stenotic lesion of the LAD was initiated.

The first step involved functional ischaemia evaluation of the LAD stenosis, which revealed a resting full-cycle ratio of 0.79 and a pressure gradient of 0.1 at the site of the eccentric calcified lesion ([Figure 1C](#)). PCI was performed using a 7 F guide catheter. Pre-intervention OCT (Dragonfly OpStar; Abbott Vascular, Santa Clara, CA, USA) showed semi-peripheral NC in the stenotic lesion (see [Supplementary material online, Video S1; Figure 2A](#)). Debulking with the Diamondback 360 coronary orbital atherectomy system (OAS) (Cardiovascular Systems, St. Paul, MN, USA) was performed three times at low speed (80 000 rpm). After OCT evaluation, an additional atherectomy was performed at a higher rotational speed (120 000 rpm). Optical coherence tomography images after high-speed atherectomy showed that the NC lesions were effectively resected, with discontinuity of the overlying superficial cap. Surprisingly, however, new granular and filamentous structures were observed proximal to the target lesions, which resembled sea anemone tentacles (a CN-like OCT finding; see [Supplementary material online, Video S2; Figure 2B](#)).

The electrocardiogram was unchanged, the TIMI flow grade was 3, and there was no evidence of slow flow or distal embolization. These very unusual tentacle-like structures appeared to be continuous from the debulked small NC lesion proximal to the target site, and OCT observation after dilatation with a 3.0 mm diameter scoring balloon (NSE Alpha; Goodman, Nagoya, Japan) revealed that although the lumen was fully dilated, extensive medial dissection had occurred and the structures appeared to have migrated somewhat distally (see [Supplementary material online, Video S3; Figure 2C](#)). A DES (Xience Skypoint 3.0 mm  $\times$  23 mm; Abbott Vascular) was implanted to cover

the entirety of these structures, with no resulting complications. Optical coherence tomography showed adequate stent expansion and granular filamentous-like structures crimped to the outside of the stent (see [Supplementary material online, Video S4; Figure 2D](#)). Because of the TIMI3 flow without distal embolization, no additional anticoagulation agents or vasodilators were administered post-operatively, and there were no perioperative elevations in myocardial enzymes. The patient was discharged uneventfully.

At a 4-month follow-up, the patient was asymptomatic but showed in-stent restenosis (ISR) on CAG ([Figure 2E](#)). Optical coherence tomography and intravascular ultrasound (IVUS) were performed to evaluate the mechanism of ISR ([Figure 2E1–5 and E1'–5'](#)). The granular and filamentous sea anemone tentacle-like structures seen at the time of initial PCI and crimped by the stent were no longer present on follow-up OCT (see [Supplementary material online, Video S5](#)). Heterogeneous severe intimal hyperplasia and organized thrombi were observed from the proximal to the mid portion of the stent, where the nodule protruded from the stent strut, and balloon dilation caused medial dissection. The distal stent sites with the crimped sea anemone tentacle-like structures contained distal NC lesions that became elliptical stent expansions. However, no restenosis was observed. Reintervention with a 3.0 mm diameter scoring balloon (Aperta NSE; Goodman) and a 3.0 mm  $\times$  25 mm drug-coated balloon (SeQuent Please; B.Braun, Berlin, Germany) was performed and successfully dilated the ISR lesion.

## Discussion

We experience a haemodialysis patient with a stable NC lesion in the LAD in which debulking using OAS disrupted the overlying superficial fibrous cap and caused the appearance of granular and filamentous-like structures on OCT, which resembled a CN. Schematic images are presented in [Figure 3](#). Calcified nodule is an infrequent but important pathological condition that can occasionally cause ACS. The recent development of OCT has provided an opportunity to better understand this condition.<sup>1</sup> Torii *et al.*<sup>2</sup> hypothesized that disruption of the fibrous cap and subsequent thrombosis in CN is initiated by the fragmentation of the calcified necrotic core via external mechanical forces in the coronary arteries in which hinge motion or excessive torsion is apparent. In the present patient, the OCT findings of tentacle-like structures were characterized by low backscatter with many contiguous small granular structures without signal-free shadowing, which are likely white platelets/fibrin thrombi.<sup>3</sup>

To our knowledge, there is only one case report of similar signal-rich dots with little attenuation on OCT.<sup>4</sup> In that study, a white web-like constitution floating in the lumen was visualized by angioscopy, which was considered a fibrin thrombus based on its morphological characteristics. Note that those findings were observed after implantation of two stents into a non-calcified tandem lesion with stable angina pectoris. Although the patient background and lesion characteristics were different from those in the present case, the OCT findings were very similar. Thus, speculatively, the sanding of the NC lesion by OAS may have caused disruption of the fibrous cap and thrombus formation, which resulted in a CN-like morphology. If this was initially identified as a thrombus, we may have changed the treatment strategy to thrombus aspiration or enhanced anticoagulation during and after PCI. However, because the identity of this OCT-observed structure could not be clarified during PCI, we made a quick decision to crimp it with a stent. Morphological evaluation with other modalities (e.g. IVUS, angioscopy, and pathologically with thrombus aspiration) would have aided with identification.

Regarding the relationship between NC and CN, CN is described as 'eruptive' and may be an early stage NC lesion with an intraplaque haemorrhage and a lipid core, while NC is described as 'non-eruptive' and may be a more mature lesion with a healed eruptive CN.<sup>2,5</sup> Indeed,



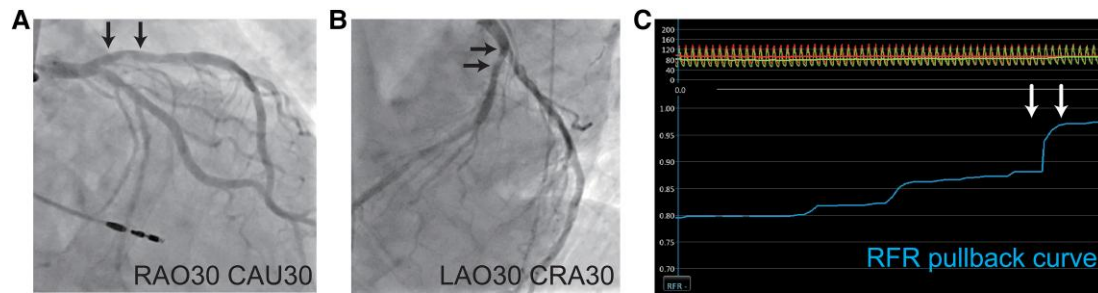


**Figure 1** (A, B) Coronary angiography showed severe stenosis with heterocentric calcification (black arrow) in the proximal left anterior descending artery. (C) The resting full-cycle ratio was 0.79, and the pressure gradient at the stenotic site was 0.1 (white arrow).

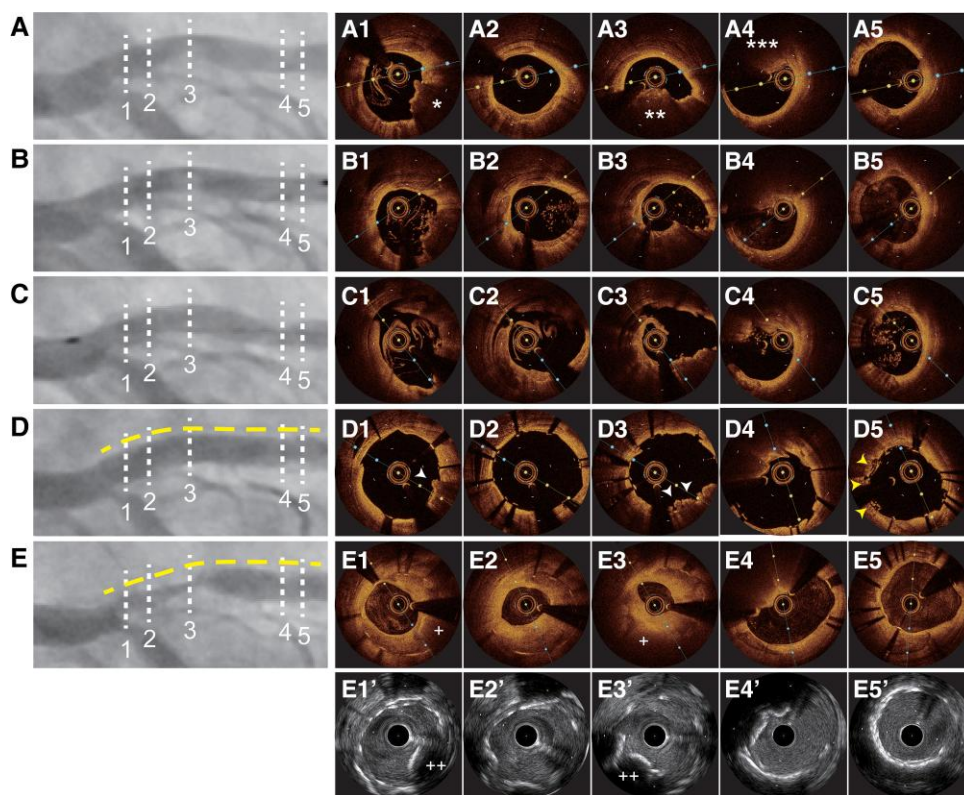


**Figure 2** (A) Pre-intervention coronary angiography (CAG) in the proximal left anterior descending artery (LAD). (A1–A5) Optical coherence tomography (OCT) images showed proximal small nodular calcification (NC) (A1, asterisk), mild stenosis with sheet calcification (A2), target NC (A3, double asterisk; the minimum luminal area was 2.96 mm<sup>2</sup>, and the calcium score of the target lesion based on OCT was calculated as 2 points for lesion length and calcium thickness), distal small NC (A4, triple asterisk), and a distal reference site with sheet calcification (A5). (B) CAG after high-speed retrograde orbital atherectomy. (B1–B5) OCT images showed newly emerged granular structures at the proximal small NC (B1, B2), effective ablation of the target NC (B3), and untreated lesions not debulked with orbital atherectomy (B4, 5). (C) CAG after dilatation of the scoring balloon. (C1–C5) OCT images showed extensive medial dissection (C1–C3), and the granular structures appeared to have migrated distally (C4, 5). (D) CAG after implantation of an everolimus-eluting stent (dotted line). (D1–D5) OCT images showed in-stent calcified nodule (CN) protrusion (D1, 3, arrowhead), good circular stent expansion (D2), elliptical stent expansion with a minimum stent area of 6.59 mm<sup>2</sup> (D3, 4), and granular structures trapped by the stent (D5, arrowhead). (E) CAG at 4 months after percutaneous coronary intervention. In-stent restenosis (ISR) was observed from the proximal to the mid portion of the stent (dotted line). (E1–5, E1'–5') High backscatter attenuation (E1, E3, crosses) on OCT and acoustic shadows (E1', E3', white double crosses) on intravascular ultrasound (IVUS) were seen at the restenosis site, which is consistent with protruding in-stent CNs. Heterogeneous neointimal hyperplasia and organized thrombi were observed at the ISR lesion (E1–3, E1'–3'), where medial dissection after balloon dilatation and CN protrusion through the stent struts were observed at the initial PCI. At the distal stent site, the stent shape was elliptical because of the NC, although no restenosis was observed (E4, E4'). Granular structures crimped by the stent were unclear (E4, 5, E4', 5').

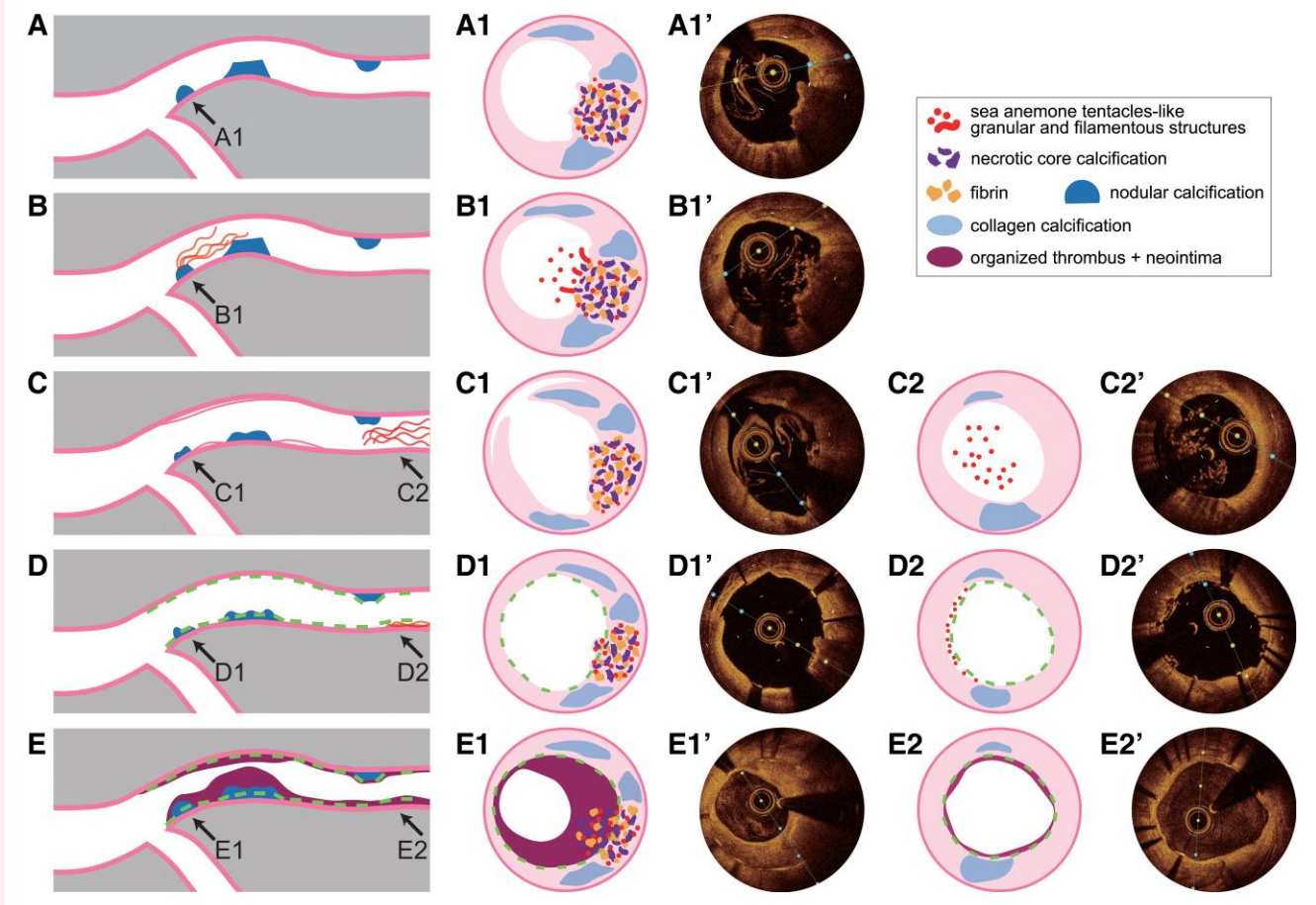


**Figure 3** Schematic images of coronary angiography and representative optical coherence tomography (OCT) cross sections of the black arrow. (A) Prior to percutaneous coronary intervention. (A1) Proximal small-sized nodular calcification (NC). (A1') Cross-sectional image of the same OCT as Figure 2A1. (B) After high-speed retrograde orbital atherectomy. (B1) New granular and filamentous structures that looked like sea anemone tentacles appeared proximal to the target NC lesions. (B1') Cross-sectional image of the same OCT as Figure 2B1. (C) After dilatation with a scoring balloon. (C1) Medial dissection was formed by balloon dilatation. (C1') Cross-sectional image of the same OCT as Figure 2C1. (C2) The sea anemone tentacle-like granular and filamentous structures appeared to have migrated distally. (C2') Cross-sectional image of the same OCT as Figure 2C5. (D) After implantation of an everolimus-eluting stent. (D1) The stent was roundly expanded with in-stent CN protrusion. (D1') Cross-sectional image of the same OCT as Figure 2D1. (D2) The sea anemone tentacle-like structures were trapped by the stent. (D2') Cross-sectional image of the same OCT as Figure 2D5. (E) In-stent restenosis occurred after 4 months. (E1) Organized thrombi and neointimal proliferation with in-stent CN protrusion were observed in the stent. (E1') Cross-sectional image of the same OCT as Figure 2E1. (E2) The sea anemone tentacle-like structures were unclear, and a thin neointima had formed. (E2') Cross-sectional image of the same OCT as Figure 2E5.

these differences in lesion morphology between 'eruptive' and 'non-eruptive' CNs as classified by OCT can cause significant differences in the degree of stent expansion and clinical outcomes, especially in target lesion revascularization (TLR).<sup>5</sup> Unfortunately, our patient also experienced TLR due to early restenosis despite relatively good stent expansion, which is consistent with the degree of stent expansion and frequent revascularization outcomes reported after stenting for 'eruptive' CNs.<sup>5</sup> The formation of severe medial dissection, which was reported to be a determinant of stent restenosis and TLR in calcified lesions,<sup>6</sup> and CN protrusion through the stent struts as an early stent restenosis factor in haemodialysis patients<sup>7</sup> are findings consistent with our patient.

We also observed a sea anemone tentacle-like structure that appeared to be a fibrin thrombus crimped distal to the stent. However, this site had no restenosis, and the finding did not appear to affect the outcome. Calcified nodules have a high incidence of subsequent

major adverse cardiac events, irrespective of whether they are treated as culprit or untreated non-culprit lesions in ACS.<sup>8,9</sup> The EROSION trial suggested that identification of the culprit lesion morphology in ACS during OCT-guided PCI may help determine a PCI strategy, especially a stentless treatment for plaque erosion.<sup>10</sup> Nevertheless, the optimal treatment strategy for CN remains unclear. Our patient underwent stent implantation because of severe medial dissection after balloon dilatation and to cover the thrombus-like structures. However, a stentless strategy may have been a better choice for initial CN treatment because of concerns over potential future stent-related adverse events and to leave the potential for debulking in subsequent treatments. A case report by Nishi *et al.*<sup>11</sup> using OCT and NIRS-IVUS suggested that the underlying necrotic core of CNs may be further increased by continued mechanical stress, which leads to luminal narrowing with lipid accumulation and immune cell infiltration, and that intense lipid-lowering and anti-inflammatory therapies are potential

treatment options to stabilize CNs. Further studies on the optimal treatment strategy for CNs, including PCI and adjunctive therapies, are warranted.

In conclusion, we experienced a haemodialysis patient with OAS de-bulking of an NC, which was considered a stable lesion, and presented with OCT findings indicative of a thrombus with superficial disruption (this closely resembled a CN). Although NCs and CNs have distinctly different pathological lesion morphologies, this is the first report suggesting that they may be transitional pathologies. Considering the limitation that OCT cannot strictly distinguish between NCs and CNs, it is also possible that lesions considered stable NCs may be in a relatively immature stage, and that the maturity of the NC lesions and the lateral sanding style of the OAS may have contributed to our striking OCT findings.

## Lead author biography



Mayuko Imamura graduated from the Faculty of Medicine, Okayama University in 2018. She is a general cardiology physician in the Department of Cardiovascular Medicine, Tsuyama Chuo Hospital, Okayama, Japan.

## Supplementary material

[Supplementary material](#) is available at *European Heart Journal – Case Reports online*.

## Acknowledgements

We thank Edanz (<https://jp.edanz.com/ac>) for editing a draft of the manuscript.

**Consent:** The authors confirm that written consent for submission and publication of this case report, including images and asso-

ciated text, has been obtained from the patient in line with COPE guidance.

**Conflict of interest:** None declared.

**Funding:** None declared.

## Data availability

The data underlying this article are available in the article and in its online [Supplementary material](#).

## References

1. Lee T, Mintz GS, Matsumura M, Zhang W, Cao Y, Usui E, et al. Prevalence, predictors, and clinical presentation of a calcified nodule as assessed by optical coherence tomography. *JACC Cardiovasc Imaging* 2017;**10**:883–891.
2. Torii S, Sato Y, Otsuka F, Kolodgie ED, Jinnouchi H, Sakamoto A, et al. Eruptive calcified nodules as a potential mechanism of acute coronary thrombosis and sudden death. *J Am Coll Cardiol* 2021;**77**:1599–1611.
3. Kume T, Akasaka T, Kawamoto T, Ogasawara Y, Watanabe N, Toyota E, et al. Assessment of coronary arterial thrombus by optical coherence tomography. *Am J Cardiol* 2006;**97**:1713–1717.
4. Osanai Y, Kurihara O, Kobayashi N, Takano M, Miyauchi Y. Unusual intracoronary structure mimicking stent deformation: observation by multimodality imaging. *JACC Cardiovasc Interv* 2023;**16**:861–862.
5. Sato T, Matsumura M, Yamamoto K, Shlofmitz E, Moses JW, Khaliq OK, et al. Impact of eruptive vs noneruptive calcified nodule morphology on acute and long-term outcomes after stenting. *JACC Cardiovasc Interv* 2023;**16**:1024–1035.
6. Torii S, Jinnouchi H, Sakamoto A, Mori H, Park J, Amoa FC, et al. Vascular responses to coronary calcification following implantation of newer-generation drug-eluting stents in humans: impact on healing. *Eur Heart J* 2020;**41**:786–796.
7. Nakamura N, Torii S, Tsuchiya H, Nakano A, Oikawa Y, Yajima J, et al. Formation of calcified nodule as a cause of early in-stent restenosis in patients undergoing dialysis. *J Am Heart Assoc* 2020;**9**:e016595.
8. Kondo S, Mizukami T, Kobayashi N, Wakabayashi K, Mori H, Yamamoto MH, et al. Diagnosis and prognostic value of the underlying cause of acute coronary syndrome in optical coherence tomography-guided emergency percutaneous coronary intervention. *J Am Heart Assoc* 2023;**12**:e030412.
9. Xu Y, Mintz GS, Tam A, McPherson JA, Iñiguez A, Fajadet J, et al. Prevalence, distribution, predictors, and outcomes of patients with calcified nodules in native coronary arteries: a 3-vessel intravascular ultrasound analysis from Providing Regional Observations to Study Predictors of Events in the Coronary Tree (PROSPECT). *Circulation* 2012;**126**:537–545.
10. Jia H, Dai J, Hou J, Xing L, Ma L, Liu H, et al. Effective anti-thrombotic therapy without stenting: intravascular optical coherence tomography-based management in plaque erosion (the EROSION study). *Eur Heart J* 2017;**38**:792–800.
11. Nishi T, Sasahira Y, Kume T, Koto S, Uemura S. Rapid progression of calcified nodules with increased lipid core burden in the right coronary artery. *Cardiovasc Interv Ther* 2023;**38**:248–250.